MCB
Journals.ASM.org

Wnt7a Regulates Multiple Steps of Neurogenesis

Qiuhao Qu, Guoqiang Sun, Kiyohito Murai, Peng Ye, Wendong Li, Grace Asuelime, Yuen-Ting Cheung, Yanhong Shi

Department of Neurosciences, Beckman Research Institute of City of Hope, Duarte, California, USA

Although Wnt7a has been implicated in axon guidance and synapse formation, investigations of its role in the early steps of neurogenesis have just begun. We show here that Wnt7a is essential for neural stem cell self-renewal and neural progenitor cell cycle progression in adult mouse brains. Loss of Wnt7a expression dramatically reduced the neural stem cell population and increased the rate of cell cycle exit in neural progenitors in the hippocampal dentate gyrus of adult mice. Furthermore, Wnt7a is important for neuronal differentiation and maturation. Loss of Wnt7a expression led to a substantial decrease in the number of newborn neurons in the hippocampal dentate gyrus. Wnt7a$^{-/-}$ dentate granule neurons exhibited dramatically impaired dendritic development. Moreover, Wnt7a activated β-catenin and its downstream target genes to regulate neural stem cell proliferation and differentiation. Wnt7a stimulated neural stem cell proliferation by activating the β-catenin–cyclin D1 pathway and promoted neuronal differentiation and maturation by inducing the β-catenin–neurogenin 2 pathway. Thus, Wnt7a exercised critical control over multiple steps of neurogenesis by regulating genes involved in both cell cycle control and neuronal differentiation.

The discovery that neurogenesis occurs in the adult brain led to the recognition of adult neural stem cells. Neural stem cells are defined as a subset of undifferentiated precursors that retain the ability to proliferate and self-renew and have the capacity to differentiate into both neuronal and glial lineages (1). Under normal conditions, neurogenesis in the adult mammalian brain is restricted to two discrete germinal centers: the subgranular layer of the hippocampal dentate gyrus and the subventricular zones of the lateral ventricles.

Wnt signaling is a key pathway that is involved in the development of the nervous system. The role of Wnt signaling in the expansion of neural progenitor cells in the developing nervous system has been studied extensively (2–7). Transgenic mice that express a constitutively active β-catenin develop larger brains, due to increased reentry of the transgenic neural precursors into the cell cycle (2, 6). Consistent with this observation, Wnt7a and Wnt7b have been shown to stimulate the proliferation of neural progenitors derived from embryonic mouse brains (4). Recently, it has been shown that Wnt7a increases both neonatal neural progenitor cell proliferation and the number of neurons derived in an *in vitro* differentiation assay (8), while treatment with Wnt3a stimulates the self-renewal divisions of neural stem cells (9). In contrast, knockout of Wnt3a or the low-density lipoprotein receptor-related protein 6 (LRP6), a Wnt receptor, leads to the loss of hippocampal progenitors and abnormal hippocampal development (3, 7). Moreover, transgenic overexpression of axin, a negative regulator of β-catenin, impairs midbrain development, due to a loss of mitotic neural precursors in the transgenic brains (5), which is similar to the neural phenotypes induced by ablation of β-catenin (6).

More recently, the function of Wnt signaling in neural stem cell proliferation and neurogenesis in adult brains has begun to be characterized (10–14). Viral transduction of a constitutively active β-catenin, or inhibition of glycogen synthase kinase 3β (GSK3β), promotes the proliferation of neural precursors in the subventricular zones of adult mouse brains, whereas genetic deletion of Wnt7a, or viral transduction of axin, decreases neural stem/progenitor cell proliferation in the hippocampal dentate gyrus and the subventricular zones, the two adult neurogenic areas (10, 14). In addition to the critical role of Wnt/β-catenin in stimulating neural stem cell proliferation and self-renewal, Wnt signaling also regulates adult neurogenesis by inducing neuronal differentiation in the hippocampus of adult mouse brains (13).

Wnt7a is a member of the Wnt family of signaling molecules. Wnt7a-knockout mice were generated by homologous recombination in mouse embryonic stem cells (15). Homozygous Wnt7a$^{-/-}$ mice are viable but exhibit defects in limb patterning (15) and female reproductive duct development (16, 17), the latter of which leads to the sterility of these animals (17). By use of the knockout mouse model, Wnt7a has been shown to play an important role in axon development, guidance, and synapse formation (18–23). Wnt7a induces axonal remodeling and synaptogenesis in cerebellar granule cells and in adult hippocampal neurons (21–23). Specifically, Wnt7a stimulates the presynaptic assembly, triggers synaptic vesicle cycling, and increases neurotransmitter release (18, 19). In addition, Wnt7a signaling promotes dendritic spine growth and excitatory synaptic strength by activating calmodulin-dependent protein kinase II (CaMKII) (20). However, a lot less is known about the role of Wnt7a signaling in the early steps of neurogenesis, including neural stem cell self-renewal, neural progenitor cell cycle progression, and neuronal differentiation and maturation, especially dentate granule neuron dendritic arborization. In this study, we examined neural stem cell self-renewal, neural progenitor cell cycle progression, and neuronal differentiation and maturation in wild-type (WT) and Wnt7a$^{-/-}$ adult mouse brains. We show that loss of Wnt7a expression led to reduced neural stem cell self-renewal, an increased rate of cell cycle exit in neural progenitors, and decreased neuronal differentiation and maturation.

Received 17 March 2013 **Returned for modification** 10 April 2013
Accepted 22 April 2013
Published ahead of print 29 April 2013
Address correspondence to Yanhong Shi, yshi@coh.org.

doi:10.1128/MCB.00325-13

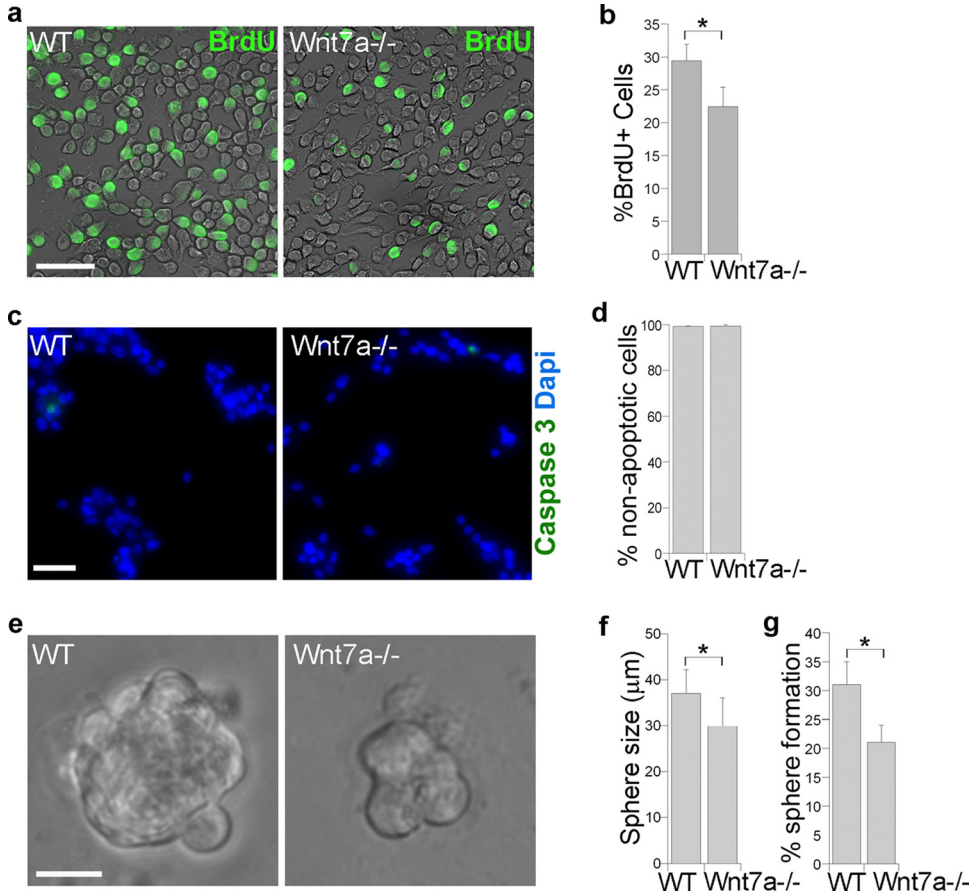

FIG 1 Loss of Wnt7a expression reduced neural stem/progenitor cell (collectively referred to as NSC) proliferation and self-renewal *in vitro*. (a) Reduced cell proliferation in NSCs isolated from Wnt7a$^{-/-}$ mouse brains. BrdU labeling (shown in green) of NSCs isolated from 6-week-old WT and Wnt7a$^{-/-}$ mouse brains. Bar, 50 μm. (b) Quantification of the percentage of BrdU-positive cells (BrdU^{+}) out of total living cells for WT and Wnt7a$^{-/-}$ NSCs after treatment with BrdU for 1 h. *, $P < 0.001$ by Student's *t* test. Experimental repeats (n) = 6. (c) Staining of both WT and Wnt7a$^{-/-}$ NSCs with active caspase-3 (shown in green). Nuclear 4′,6-diamidino-2-phenylindole (DAPI) staining is shown in blue. Bar, 50 μm. (d) Quantification of nonapoptotic cells in WT and Wnt7a$^{-/-}$ NSCs. The nonapoptotic cells were negative for active caspase-3 staining. $n = 3$. (e) Images of representative neurospheres of WT and Wnt7a$^{-/-}$ NSCs from clonal analysis. Bar, 20 μm. (f) Quantification of WT and Wnt7a$^{-/-}$ neurosphere size. *, $P < 0.005$ by Student's *t* test. (g) Quantification of WT and Wnt7a$^{-/-}$ neurosphere formation rate. *, $P < 0.001$ by Student's *t* test. Error bars are standard deviations of the means for all the quantification data. $n = 6$ (f and g).

MATERIALS AND METHODS

Immunostaining and quantification. Immunostaining was carried out on 20- or 40-μm brain sections or cultured cells using antibodies, including rat antibromodeoxyuridine (anti-BrdU) (Accurate; 1:5,000), mouse anti-Ki67 (Lab Vision; 1:400), rabbit anti-Tuj1 (Covance; 1:5,000), mouse anti-glial fibrillary acidic protein (anti-GFAP) (Sigma; 1:1,000), mouse anti-O4 (Sigma; 1:400), mouse anti-Map2 (Sigma; 1:600), goat anti-Sox2 (Santa Cruz; 1:100), and goat antidoublecortin (anti-DCX) (Santa Cruz; 1:200). Images were visualized by a Zeiss confocal or inverted microscope. *In vivo* BrdU labeling was performed as described previously (24). For BrdU and DCX double labeling, mice were injected with BrdU intraperitoneally once daily at 50 mg/kg of body weight for 7 days. Brains were harvested 3 weeks later for BrdU and DCX costaining. For quantification, every eighth section of slides per animal (about 8 sections per brain), including the hippocampal dentate gyrus region, was selected. The dentate gyri were scanned using a confocal microscope. Z series of confocal images were captured. The number of single- or double-stained cells was counted.

For analysis of dendritic development *in vivo*, a three-dimensional (3D) reconstruction of entire dendritic processes of neurons was made from Z stacks of confocal images. The two-dimensional (2D) projection images were traced with NIH Image J. Dentate granule cells with largely intact dendritic trees were analyzed for total dendritic length as described previously (25). Dendritic complexity was measured using Sholl analysis plugged into NIH Image J by counting the number of dendrites that cross a series of concentric circles from the cell soma as described previously (25). A minimum of 10 neurons from randomly picked sections per animal and six animals was analyzed for neuronal morphology under each condition. Two-way analysis of variance (ANOVA) was used for statistical analysis.

Neural stem cell culture, proliferation, differentiation, and self-renewal analysis. Mouse neural stem cells were isolated from 6-week-old WT or Wnt7a$^{-/-}$ brains (Jackson Laboratory) using methods modified from published protocols (24, 26). Specifically, adult mouse forebrains containing the hippocampal dentate gyri and subventricular zones were sliced into 400-μm sections. Brain tissues were dissociated using the MACS neural dissociation kit (Miltenyi). Dissociated cells were centrifuged in a 10% Percoll solution in phosphate-buffered saline (PBS). Cells were collected and plated in neurobasal medium containing 2% B27, 1% glutamine, 20 ng/ml epithelial growth factor (EGF), and fibroblast growth factor 2 (FGF2). Newly formed neurospheres were dissociated into single cells using trypsin and transferred into Dulbecco's modified Eagle medium (DMEM)–F-12 medium supplemented with N2, 20 ng/ml EGF and FGF2, and 5 μg/ml heparin and cultured in this medium for further passages.

BrdU labeling was performed to monitor neural stem cell proliferation

by treating neural stem cells with 10 μM BrdU for 1 h. The BrdU-treated cells were HCl treated, followed by BrdU antibody staining. Clonal analysis was performed by dissociating neurospheres into single cells and plating them at one cell per well in 96-well plates. These cells were cultured for 2 weeks to allow primary neurosphere formation. The primary neurospheres were dissociated into single cells and seeded at 50 cells per well in 96-well plates to allow secondary sphere formation. Data presented are secondary sphere size and formation rate.

For differentiation assays, neural stem cells were dissociated into single cells and cultured in DMEM–F-12 medium, supplemented with N2, 1 μM retinoic acid (RA), and 0.5% fetal bovine serum (FBS). Three days after differentiation, cells were immunostained for Tuj1, GFAP, and O4. The Tuj1-positive, GFAP-positive, or O4-positive cells were counted and calculated for the percentage of Tuj1-positive, GFAP-positive, or O4-positive cells. More than 5,000 cells were counted for each experiment. To measure dendritic length and complexity of differentiated neurons, neural stem cells were differentiated in the same differentiation medium for 5 days. Dendritic length was measured using NIH Image J. Dendritic complexity was measured using Sholl analysis plugged into NIH Image J.

***In vivo* cell cycle analysis.** Six-week-old WT and Wnt7a$^{-/-}$ littermate mice were injected with BrdU intraperitoneally at 50 mg/kg of mouse body weight, and animals were allowed to survive for 30 min or 24 h. Brains of the treated animals were collected for cell cycle analysis as described previously (27). For cell cycle length analysis, mice were treated with BrdU for 30 min, followed by BrdU and Ki67 double staining of brain sections. The fraction of progenitor cells in S phase, a labeling index, was determined by scoring the percentage of BrdU-labeled neural progenitor cells (BrdU$^+$ Ki67$^+$/Ki67$^+$). This labeling index provides an estimation of cell cycle length. Decreased labeling index suggests lengthened cell cycles. For cell cycle reentry analysis, mice were treated with BrdU for 24 h, followed by BrdU and Ki67 double staining of brain sections. Cells that left the cell cycle were identified as BrdU$^+$ and Ki67$^-$, and cells that reentered the cell cycle were identified as BrdU$^+$ and Ki67$^+$. Percentage of cell cycle reentry was expressed as BrdU$^+$ Ki67$^+$/BrdU$^+$ cells.

Apoptosis assay. We used the active form of caspase-3 as an indicator for apoptosis. Immunostaining was used to detect active caspase-3 in both WT and Wnt7a$^{-/-}$ neural stem cells by incubation with an antibody specific for the cleaved, active caspase-3 (Cell Signaling; 1:100), followed by incubation with the fluorescein isothiocyanate (FITC)-conjugated secondary antibody.

Viral vector construction, viral preparation, and transduction. The DNA sequence containing the Wnt7a small interfering RNA (siRNA) was inserted into the pHIV lentiviral vector with a puromycin resistance gene. The neurogenin 2 (Ngn2) lentivirus vector (Addgene plasmid 34999) was purchased from Addgene. The constitutively active β-catenin that lacks its amino-terminal 90 amino acids was cloned into the NIT retroviral vector as described previously (14). Viral preparation and transduction were performed as previously described (14).

Real-time RT-PCR analysis. Total RNA was purified using TRIzol reagent (Invitrogen). Reverse transcription was performed with 1 μg of RNA using the Omniscript reverse transcription kit (Qiagen). Real-time reverse transcription-PCR (RT-PCR) was performed using iTaq SYBR green Supermix with 5-carboxy-*X*-rhodamine (ROX) (Bio-Rad) in an Applied Biosystems Step One Plus real-time PCR system. The primers for RT-PCR included the following: Wnt7a forward, 5′ CTG TGG CTG CGA CAA GGA GA 3′; Wnt7a reverse, 5′ TGG CAC GCA CAG GCT CCA CGT GG 3′; cyclin D1 forward, 5′ GAG ACC ACA GCC CTC CCC AGA CGG 3′; cyclin D1 reverse, 5′ AAG CGG TCC AGG TAG TTC ATG G 3′; Ngn2 forward, 5′ TCG TCA AAT CTG AGA CTC TGG AG 3′; Ngn2 reverse, 5′ CGG CGC AGC TCC TCG TCC T 3′; β-actin forward, 5′ CCG AGC GTG GCT ACA GCT TC 3′; and β-actin reverse, 5′ ACC TGG CCG TCA GGC AGC TC 3′.

ChIP assays. We performed chromatin immunoprecipitation (ChIP) assays using the EZ-ChIP kit (Millipore) with precleaned chromatin from 2×10^6 mouse neural stem cells and 5 μg antibody for each ChIP assay using antibodies for β-catenin (BD BioScience; 610153), acetylated histone H3 (AcH3) (Millipore; 06-599), and trimethylated histone H3 lysine 4 (H3K4me3) (Abcam; Ab8580). Mouse IgG (IgG1) and rabbit IgG (IgG2) were included as the negative controls. The primers for ChIP assays included the following: cyclin D1 F, 5′ AGG GAC TTC AAC ATA AAT CAT GC 3′; cyclin D1 R, 5′ GCA CCA CCA TAC CCA GCA TAT GC 3′; Ngn2 F, 5′ CTG ACA CAG CAG GTT CCT CTC AT 3′; and Ngn2 R, 5′ AGC ATT GAG ACC AAA CAC TTA AC 3′.

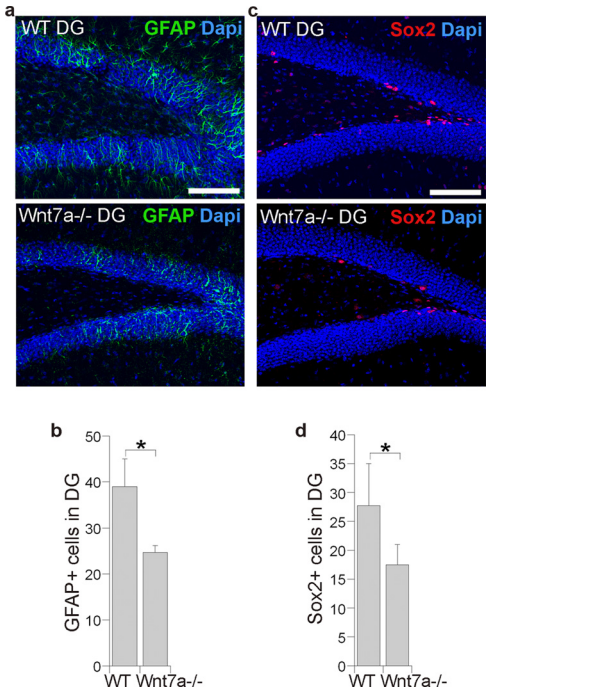

FIG 2 Reduced neural stem cell population in the hippocampal dentate gyrus (DG) of Wnt7a$^{-/-}$ adult mouse brains. (a) Immunostaining of the hippocampal dentate gyrus of 6-week-old WT and Wnt7a$^{-/-}$ mice for GFAP (green). Nuclear DAPI staining is shown in blue. (b) Quantification of GFAP$^+$ cells per 40-μm section in the hippocampal dentate gyrus of 6-week-old WT and Wnt7a$^{-/-}$ mice. (c) Immunostaining for Sox2 (red) in the hippocampal dentate gyrus of 6-week-old WT and Wnt7a$^{-/-}$ mice. (d) Quantification of Sox2$^+$ cells per 40-μm section in the hippocampal dentate gyrus of 6-week-old WT and Wnt7a$^{-/-}$ mice. Error bars are standard deviations of the means. *, $P < 0.05$ by Student's *t* test for (b and d). Bar, 100 μm (a and c). $n = 3$ for both WT and Wnt7a$^{-/-}$ mice (b and d).

Golgi staining. Golgi staining was performed as described previously (28). Briefly, brains were taken from freshly blood-drained animals, fixed in 4% paraformaldehyde (PFA) overnight, and impregnated in a 5% solution of potassium dichromate at room temperature for 3 days with gentle rotating. The brains were then stained in 2% silver nitrite for 3 to 5 days with daily solution change. The stained brains were embedded in a 3% low-melting-temperature agarose gel (Sigma) and cut into 60-μm coronal sections on a vibratome. Sections were rinsed in distilled water and mounted onto glass slides with Paramount.

RESULTS

Loss of Wnt7a expression affected neural progenitor cell cycle progression. Since Wnt7a is expressed in the active adult neurogenic areas (14, 29), we tested whether loss of Wnt7a expression affects adult neural stem/progenitor cell proliferation and self-renewal. We isolated neural stem/progenitor cells from forebrains of 6-week-old WT and Wnt7a$^{-/-}$ mice and cultured these cells in DMEM–F-12 medium supplemented with N2, epithelial growth

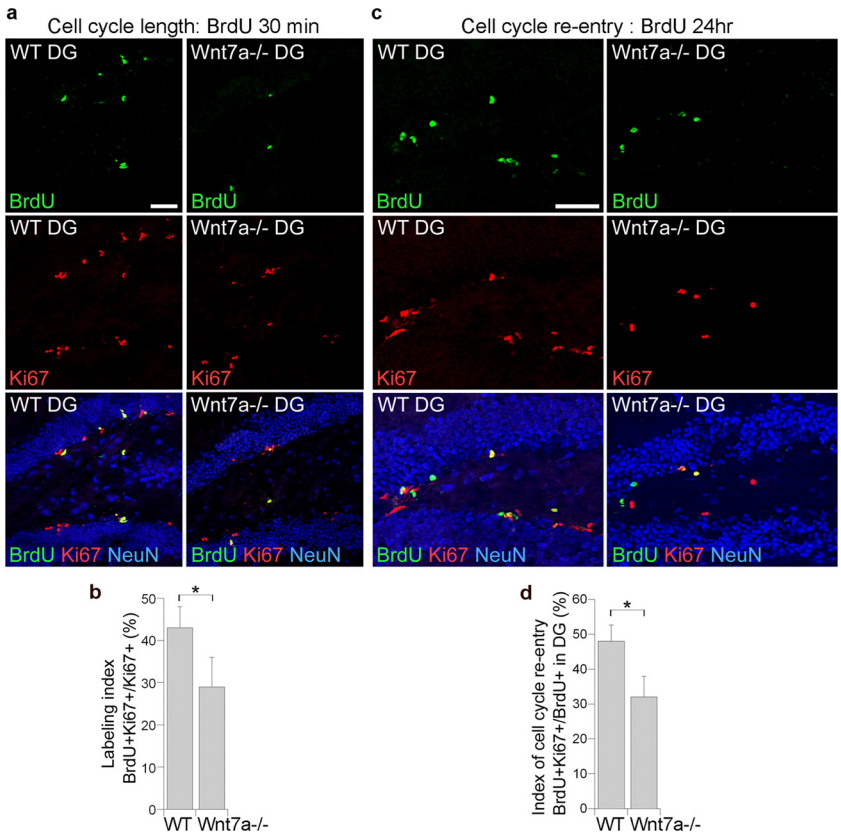

FIG 3 The Wnt7a$^{-/-}$ neural progenitors exhibited lengthened cell cycles and reduced cell cycle reentry *in vivo*. (a) Cell cycle length analysis was performed by treating 6-week-old WT and Wnt7a$^{-/-}$ mice with BrdU for 30 min before brain harvest and then double staining the hippocampal dentate gyrus (DG) with BrdU (shown in green) and Ki67 (shown in red). NeuN staining (shown in blue) was included to show the structure of the dentate gyrus. Bar, 50 μm. (b) Quantification of BrdU$^+$ Ki67$^+$ cells in total Ki67$^+$ cells in the DG. The labeling index of cell cycle length is defined as the percentage of BrdU$^+$ Ki67$^+$ cells in total Ki67$^+$ cells. Decreased labeling index suggests lengthening cell cycles. Error bars are standard deviations of the means. *, $P < 0.005$ by Student's *t* test. $n = 6$ for both WT and Wnt7a$^{-/-}$ mice. (c) Cell cycle reentry and exit analysis was performed by treating 6-week-old WT and Wnt7a$^{-/-}$ mice with BrdU for 24 h before brain harvest and then double staining the hippocampal DG with BrdU (shown in green) and Ki67 (shown in red). Bar, 50 μm. (d) Quantification of BrdU$^+$ Ki67$^+$ cells in total BrdU$^+$ cells in the DG. The index of cell cycle reentry is defined as the percentage of BrdU$^+$ Ki67$^+$/BrdU$^+$ cells. Error bars are standard deviations of the means. *, $P < 0.001$ by Student's *t* test. $n = 6$ for both WT and Wnt7a$^{-/-}$ mice.

factor (EGF), fibroblast growth factor 2 (FGF2), and heparin. Neural stem/progenitor cells were treated with BrdU for 1 h, and then cell proliferation was monitored by BrdU labeling. The number of BrdU-positive cells was dramatically reduced in Wnt7a$^{-/-}$ neural stem cells compared to WT cells (Fig. 1a and b). Minimal levels of active caspase-3, an indicator of apoptosis, were detected in both WT and Wnt7a$^{-/-}$ cells (Fig. 1c and d), suggesting that the decreased BrdU labeling in Wnt7a$^{-/-}$ cells was not due to increased apoptosis.

The self-renewal capacity of WT and Wnt7a$^{-/-}$ neural stem cells was determined by clonal analysis. Primary clonal populations were derived from single WT or Wnt7a$^{-/-}$ neural stem cells. The primary neurospheres were dissociated into single cells and plated at 50 cells per well in 96-well plates to allow secondary sphere formation. The secondary sphere size and formation rate served as an index of self-renewal ability. Loss of Wnt7a expression led to a dramatically reduced self-renewal ability in neural stem cells, as revealed by decreases in both neurosphere size and neurosphere formation rate in Wnt7a$^{-/-}$ neural stem cells, compared to WT neural stem cells (Fig. 1e to g). These results indicate that Wnt7a plays an important role in neural stem/progenitor cell proliferation and self-renewal.

In adult mammalian brains, both the GFAP-expressing radial glia-like cells and the Sox2-positive cells have been considered neural stem cells in the subgranular zone of the hippocampal dentate gyrus (30, 31). To determine if the neural stem cell population was affected by loss of Wnt7a expression, we immunostained hippocampal sections of 6-week-old WT and Wnt7a$^{-/-}$ littermate mice for GFAP and Sox2. The number of both GFAP$^+$ cells and Sox2$^+$ cells was reduced in the subgranular zone of the hippocampal dentate gyrus of Wnt7a$^{-/-}$ brains, compared to those in the corresponding region of the WT brains (Fig. 2). These results suggest that Wnt7a expression is important for maintaining neural stem cell population in the hippocampal dentate gyrus of adult mouse brains.

Next, we analyzed *in vivo* cell cycle progression of WT and Wnt7a$^{-/-}$ neural precursors in the hippocampal dentate gyrus to compare their relative cell cycle lengths. Specifically, 6-week-old WT and Wnt7a$^{-/-}$ mice were pulsed with BrdU for 30 min. Neural progenitor cells were identified by Ki67 immunoreactivity (32, 33), and cells in S phase were labeled by BrdU staining. The fraction of progenitor cells in S phase, a labeling index, was determined by calculating the percentage of BrdU-positive and Ki67-positive cells out of total Ki67-positive cells (BrdU$^+$ Ki67$^+$/

Ki67$^+$). Because the length of S phase remains relatively constant in mammalian cells, whereas the length of G_1 phase regulates proliferation (34), this labeling index provides an estimate of cell cycle length. A decreased labeling index suggests longer cell cycles (2). By examining hippocampal dentate gyrus sections from six pairs of brains, we showed that neural progenitors in the dentate gyrus of Wnt7a$^{-/-}$ adult brains divided more slowly than those in the dentate gyrus of WT littermates, as indicated by the decreased labeling index in the Wnt7a$^{-/-}$ cells (Fig. 3a and b).

In addition to cell cycle length, we also determined whether Wnt7a regulates cell cycle reentry and exit of neural progenitors in adult hippocampal dentate gyrus. Cell cycle reentry was determined by scoring the fraction of cells that reentered cell cycle after pulse-labeling with BrdU for 24 h before brain harvest. Cells that had left the cell cycle were stained as BrdU$^+$ and Ki67$^-$, whereas cells that reentered the cell cycle were stained as BrdU$^+$ and Ki67$^+$. The index of cell cycle reentry is defined as the percentage of BrdU$^+$ Ki67$^+$ cells in total BrdU$^+$ cells (35). A significant decrease in the percentage of neural progenitors that reentered the cell cycle was observed in the hippocampal dentate gyrus of Wnt7a$^{-/-}$ brains, compared to that in WT brains, indicating that loss of Wnt7a expression led to increased cell cycle exit (Fig. 3c and d). Together, these results suggest that Wnt7a is important for controlling cell cycle progression of neural progenitors in the adult hippocampus.

Loss of Wnt7a expression inhibited neuronal differentiation and maturation. To test whether Wnt7a regulates neural differentiation, we treated neural stem/progenitor cells isolated from WT or Wnt7a$^{-/-}$ adult brains with retinoic acid (RA) and fetal bovine serum (FBS) to induce differentiation. After 3 days of treatment, the differentiated cells were stained with Tuj1, a neuronal marker; GFAP, an astrocyte marker; and O4, an oligodendrocyte marker. Both WT and Wnt7a$^{-/-}$ neural stem/progenitor cells were able to differentiate into all three lineages (Fig. 4a), suggesting that both are multipotent. Interestingly, there was a substantial decrease in the percentage of Tuj1$^+$ neurons in Wnt7a$^{-/-}$ cells, compared to WT cells (Fig. 4a and b). In contrast, the GFAP$^+$ astrocytes were slightly increased in Wnt7a$^{-/-}$ cells (Fig. 4c), and we saw no significant difference in the percentages of O4$^+$ oligodendrocytes between the WT and Wnt7a$^{-/-}$ cells (Fig. 4d). These results suggest that Wnt7a is important for neuronal differentiation.

To test whether Wnt7a regulates neurogenesis *in vivo*, we treated 6-week-old WT and Wnt7a$^{-/-}$ mice with BrdU for 7 days and harvested the brains 3 weeks after BrdU treatment. Neurogenesis was monitored by BrdU and doublecortin (DCX) double staining. When quantified, the number of BrdU-positive and DCX-positive newborn neurons in the hippocampal dentate gyrus was substantially decreased in Wnt7a$^{-/-}$ brains compared to WT brains (Fig. 5a and b). Moreover, the dendritic growth of Wnt7a$^{-/-}$ neurons was dramatically impaired compared to that of WT neurons, as revealed by a considerable decrease in dendritic length (Fig. 5c and d). Sholl analysis showed substantially reduced dendritic complexity of the Wnt7a$^{-/-}$ dentate granule neurons (Fig. 5e).

The role of Wnt7a in dendritic arborization in the hippocampal dentate gyrus was further investigated using Golgi staining, a method that has been widely used for studying neuronal morphology (36). Decreases in both dendritic length and complexity were observed in the dentate granule neurons in the hippocampus of

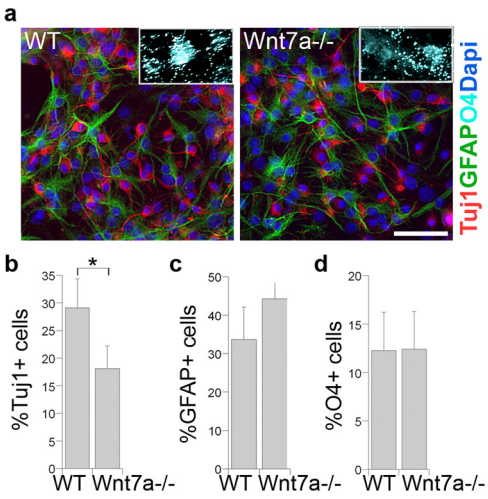

FIG 4 Loss of Wnt7a expression decreased neuronal differentiation potential and neurite complexity *in vitro*. (a) The Wnt7a$^{-/-}$ NSCs that were induced to differentiate show reduced neuronal differentiation potential, revealed by the decreased percentage of Tuj1$^+$ cells. NSCs isolated from WT or Wnt7a$^{-/-}$ mouse brains were induced to differentiate for 3 days using retinoic acid (RA) and FBS. The differentiated cells were immunostained for a neuronal marker, Tuj1 (red); an astrocyte marker, GFAP (green); and an oligodendrocyte marker, O4 (light blue, in the inset). Nuclear DAPI staining is shown in dark blue. Bar, 50 μm. (b) Quantification of Tuj1$^+$ cells in WT and Wnt7a$^{-/-}$ cells. *, $P < 0.001$ by Student's *t* test. (c and d) Quantification of GFAP$^+$ cells (c) and O4$^+$ cells (d) in WT and Wnt7a$^{-/-}$ cells. Error bars are standard deviations of the means for all quantifications. Experimental repeats (n) = 6 (b to d).

adult Wnt7a$^{-/-}$ mice, compared to those in the hippocampus of WT littermate mice (Fig. 5f, g, and h). Taken together, these results further support our hypothesis that Wnt7a plays an important role in neurogenesis by promoting both neuronal differentiation and maturation.

Wnt7a regulates neural stem/progenitor cell proliferation and neuronal differentiation by activating the expression of cyclin D1 and neurogenin 2 (Ngn2). Wnt7a is expressed in both neural stem/progenitor cells and neurons, with a relatively higher expression in neural stem/progenitor cells (Fig. 6a). We transduced both neural stem/progenitor cells and neurons with a lentiviral vector expressing a small hairpin interference RNA (siRNA) for Wnt7a. Knockdown of Wnt7a expression was evident in both neural stem/progenitor cells and neurons (Fig. 6a). Next, we tested if knockdown of Wnt7a expression affects β-catenin downstream target gene expression in neural stem/progenitor cells and neurons. We observed dramatically reduced expression of cyclin D1, a downstream target gene of β-catenin (37), in the Wnt7a knockdown neural stem/progenitor cells (Fig. 6b). The expression of cyclin D1 was relatively low in neurons, and knockdown of Wnt7a exhibited no obvious effect on the neuronal expression of cyclin D1 (Fig. 6b). In contrast, we saw a dramatic reduction in the expression of Ngn2, a proneural basic helix-loop-helix transcription factor that has been shown to promote neuronal differentiation (38–40), in Wnt7a knockdown neurons (Fig. 6c). However, there was no detectable effect on Ngn2 expression in Wnt7a knockdown neural stem/progenitor cells (Fig. 6c).

We used chromatin immunoprecipitation (ChIP) analysis to show that the Wnt downstream effector β-catenin was bound to the lymphoid enhancer binding factor (LEF)/T cell transcription factor (TCF) binding site on the cyclin D1 promoter in neural

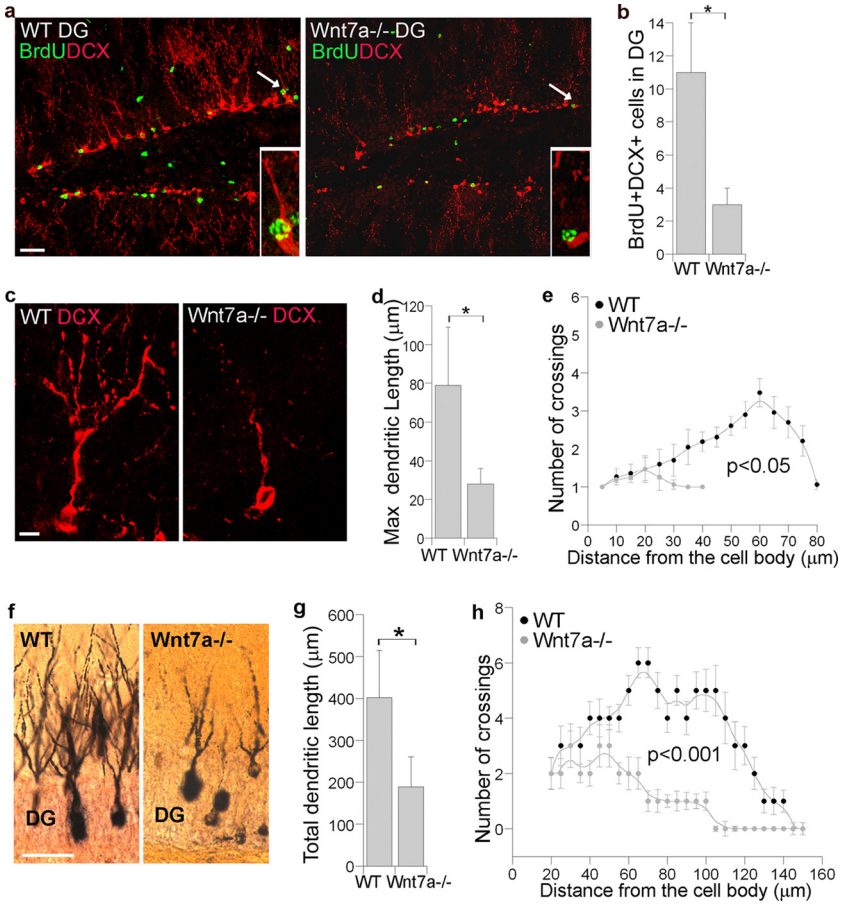

FIG 5 Loss of Wnt7a expression reduced neurogenesis and impaired dendritic arborization in dentate granule neurons *in vivo*. (a) Reduced numbers of $BrdU^+$ DCX^+ cells in the dentate gyrus (DG) of $Wnt7a^{-/-}$ brains. BrdU (green) and DCX (red) double staining in the DG of WT and $Wnt7a^{-/-}$ mouse brains from 6-week-old mice that were treated with BrdU for 1 week, followed by 3-week survival. Bar, 100 μm. The insets are enlarged images of the cells indicated by arrows. (b) Quantification of $BrdU^+$ DCX^+ cells in the DG of WT and $Wnt7a^{-/-}$ brains. The numbers represent $BrdU^+$ DCX^+ cells in the DG per 20-μm section. Error bars are standard deviations of the means. *, $P < 0.001$ by Student's *t* test. (c) Images of dendritic arborization of dentate granule neurons in age- and gender-matched WT and $Wnt7a^{-/-}$ mouse brains shown by DCX staining (red). Bar, 20 μm. (d) Quantification of the maximal (max) dendritic length of DCX-positive neurons in the DG of WT and $Wnt7a^{-/-}$ brains. Error bars are standard deviations of the means. *, $P < 0.01$ by Student's *t* test. (e) Analysis of dendritic complexity of DCX^+ dentate granule neurons in WT and $Wnt7a^{-/-}$ brains using Sholl analysis. Errors bars are standard errors of the means. *P* values were determined by 2-way ANOVA. (f) Images of dendritic arborization of dentate granule neurons in age- and gender-matched WT and $Wnt7a^{-/-}$ mouse brains shown by Golgi staining. Bar, 50 μm. (g) Quantification of total neurite length per dentate granule neuron in the hippocampal dentate gyrus of age- and gender-matched WT and $Wnt7a^{-/-}$ mice. Error bars are standard deviations of the means. *, $P < 0.001$ by Student's *t* test. (h) Analysis of dendritic complexity of dentate granule neurons revealed by Golgi staining in the DG of age- and gender-matched WT and $Wnt7a^{-/-}$ mice using Sholl analysis. Error bars are standard errors of the means. *P* values were determined by 2-way ANOVA. $n = 6$ for both WT and $Wnt7a^{-/-}$ mice for all panels.

stem/progenitor cells, and this site was associated with the active chromatin markers (Fig. 6d) acetylated histone H3 (AcH3) and trimethylated histone H3 lysine 4 (H3K4me3) (41, 42). We did not detect any β-catenin at the LEF/TCF binding site in the Ngn2 promoter in neural stem/progenitor cells (Fig. 6e). However, when neural stem/progenitor cells were induced to differentiate into neurons, β-catenin could no longer be detected at the cyclin D1 promoter (Fig. 6f). Instead, it was bound to the LEF/TCF binding site in the Ngn2 promoter, and this site was associated with the active chromatin markers AcH3 and H3K4me3 (Fig. 6g). The binding of β-catenin to the Ngn2 promoter, in combination with the previous observation that β-catenin activated a luciferase reporter gene under the control of the Ngn2 promoter (43), indicates that Ngn2 is a direct downstream target gene of β-catenin. Together, these results suggest that Wnt7a regulates neural stem/progenitor cell proliferation and neuronal differentiation by preferentially activating downstream target genes of β-catenin that are involved in cell cycle control under proliferating conditions and those involved in neuronal differentiation upon differentiation.

To further determine if Wnt7a regulates neural stem/progenitor cell proliferation by activating β-catenin and its downstream target genes, we transduced neural stem/progenitor cells with lentivirus expressing Wnt7a siRNA to knock down Wnt7a expression. Consistent with our observation that cell proliferation in neural stem/progenitor cells isolated from adult $Wnt7a^{-/-}$ mouse brains was greatly reduced (Fig. 1a and b), a dramatic decrease in BrdU labeling was observed in Wnt7a knockdown neural stem/progenitor cells (Fig. 7a and b). Cotransduction of the Wnt7a siRNA with a constitutively active β-catenin that lacks its amino-terminal 90 amino acids containing the GSK3β phosphorylation site to mimic active Wnt signaling (14) substantially restored the cell proliferation that was inhibited by the knockdown of Wnt7a

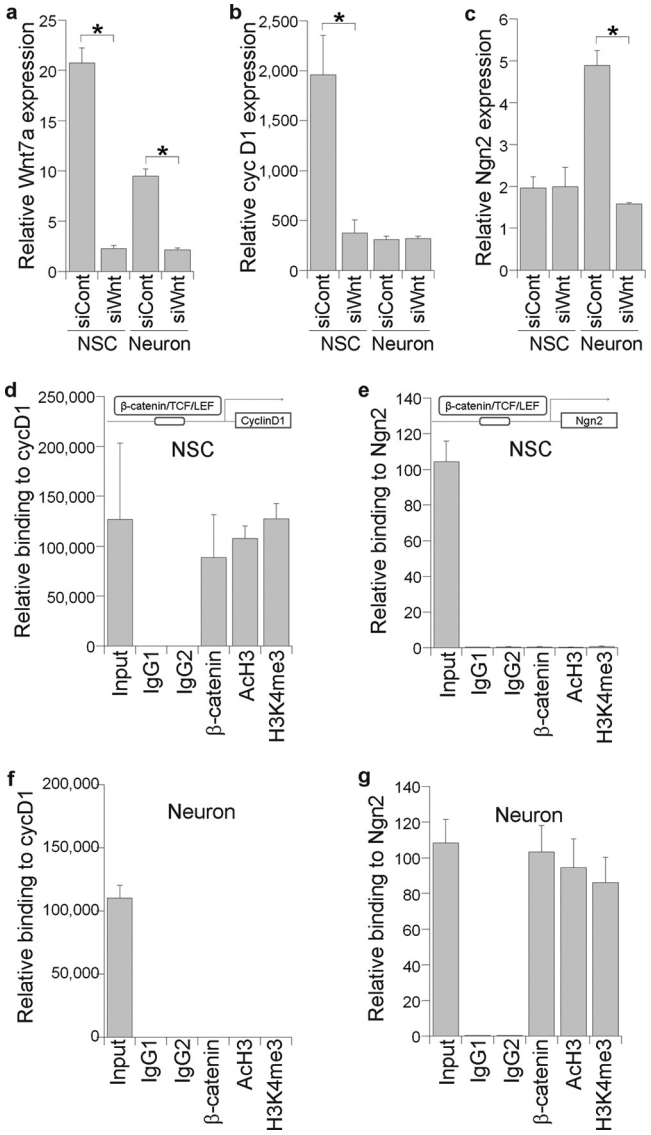

FIG 6 Wnt7a regulates cyclin D1 and Ngn2 expression. (a to c) RT-PCR analysis of Wnt7a (a), cyclin D1 (cyc D1) (b), and Ngn2 (c) expression in NSCs or neurons that were transduced with control RNA (siCont) or Wnt7a siRNA (siWnt). Error bars are standard deviations of the means. *, $P < 0.001$ by Student's *t* test (a to c). (d and e) ChIP analysis to measure the relative binding of β-catenin to the TCF/LEF binding site on the promoter of cyclin D1 (cycD1) (d) or Ngn2 (e) in NSCs. A diagram of the cyclin D1 and Ngn2 genes is shown, with the genomic region amplified for ChIP analysis indicated by an open box. (f and g) ChIP analysis to measure the relative binding of β-catenin to the TCF/LEF binding site on the promoter of cyclin D1 (cycD1) (f) or Ngn2 (g) when NSCs were induced to differentiate into neurons. For panels d to g, 10% cell lysates were included as the input. Both mouse IgG (IgG1) and rabbit IgG (IgG2) were included as the negative controls. The levels of the active chromatin markers AcH3 and H3K4me3 on the same promoters were measured in parallel. $n = 3$ for all panels. ChIP enrichment of genomic DNA for each antibody was calculated as the percentage of input in the following: $4 \times 10^{-6} \pm 1 \times 10^{-6}$ for IgG1 and IgG2, 0.23 ± 0.11 (β-catenin), 0.28 ± 0.03 (AcH3), and 0.34 ± 0.04 (H3K4me3) in panel d; 0.001 ± 0.0002 (IgG1), 0.001 ± 0.0007 (IgG2), and 0.001 ± 0.0006 for all three antibodies (β-catenin, AcH3, and H3K4me3) in panel e; 1×10^{-6} to $8 \times 10^{-6} \pm 1 \times 10^{-6}$ to 4×10^{-6} for IgG1, IgG2, and all three antibodies in panel f; 0.001 ± 0.0005 (IgG1), 0.001 ± 0.0001 (IgG2), 0.32 ± 0.05 (β-catenin), 0.29 ± 0.05 (AcH3), and 0.26 ± 0.04 (H3K4me3) in panel g.

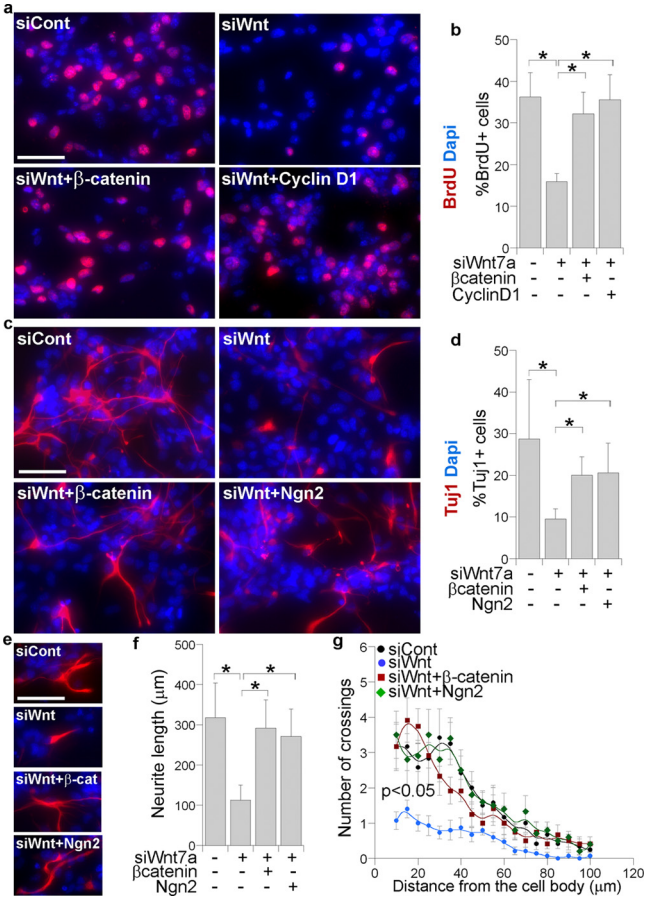

FIG 7 Wnt7a regulates NSC proliferation and neuronal differentiation by activating β-catenin and its downstream target genes. (a) NSCs were transduced with control RNA (siCont), Wnt7a siRNA (siWnt), the combination of siWnt and the constitutively active β-catenin (siWnt + β-catenin), or the combination of siWnt and cyclin D1 (siWnt + Cyclin D1). The transduced cells were treated with BrdU for 1 h. Cell proliferation was monitored by BrdU labeling, shown in red. Nuclear DAPI staining is shown in blue. Bar, 50 μm. (b) Quantification of the percentage of $BrdU^+$ cells in total living cells. Error bars are standard deviations of the means. *, $P < 0.001$ by Student's *t* test. $n = 7$. (c) NSCs were transduced with siCont, siWnt, siWnt + β-catenin, or the combination of siWnt and Ngn2 (siWnt + Ngn2) and induced to differentiate into neurons. Neuronal differentiation was monitored by immunostaining of Tuj1, shown in red. Nuclear DAPI staining is shown in blue. Bar, 50 μm. (d) Quantification of the percentage of $Tuj1^+$ cells out of the total living cells for each treatment described in panel c. Error bars are standard deviations of the means. *, $P < 0.001$ by Student's *t* test. $n = 3$. (e) Images of individual neurons derived from NSCs transduced with siCont, siWnt, siWnt + β-catenin (siWnt + β-cat), or siWnt + Ngn2. Bar, 50 μm. (f) Quantification of total neurite length per neuron shown in panel e. Error bars are standard deviations of the means. *, $P < 0.001$ by Student's *t* test. $n = 3$. (g) Analysis of dendritic complexity of $Tuj1^+$ neurons shown in panel e using Sholl analysis. Error bars are standard errors of the means. $n = 10$. *P* values were determined by 2-way ANOVA.

(Fig. 7a and b). When cyclin D1 was cotransduced with Wnt7a siRNA, there was a similar recovery of cell proliferation (Fig. 7a and b). Together, these results indicate that Wnt7a stimulates neural stem/progenitor cell proliferation by activating the β-catenin–cyclin D1 pathway.

To determine if Wnt7a regulates neuronal differentiation by activating β-catenin, we transduced neural stem/progenitor cells with Wnt7a siRNA alone, or together with the constitutively active

β-catenin. The transduced cells were then induced to differentiate into neurons. Consistent with the observed decrease in neuronal differentiation of neural stem/progenitor cells isolated from the Wnt7a$^{-/-}$ adult mouse brains (Fig. 4), the number of Tuj1^{+} neurons induced from Wnt7a knockdown neural stem/progenitor cells was dramatically reduced (Fig. 7c and d). Remarkably, cotransducing Wnt7a siRNA with the constitutively active β-catenin restored neuronal differentiation considerably. Similarly, when we cotransduced Wnt7a siRNA with Ngn2, a downstream target gene of β-catenin that is involved in neuronal differentiation, neuronal differentiation was substantially restored as revealed by the increased number of Tuj1^{+} cells (Fig. 7c and d). In addition to rescuing the reduced levels of neuronal differentiation induced by Wnt7a knockdown, both the constitutively active β-catenin and Ngn2 also restored the neuronal maturation defects induced by Wnt7a siRNA. Both neurite length and neuronal complexity recovered substantially in cells treated with the Wnt7a siRNA in combination with either the active β-catenin or Ngn2, compared to those in cells treated with Wnt7a siRNA alone (Fig. 7e, f, and g). These results together indicate that Wnt7a regulates neural stem/progenitor cell proliferation and differentiation by activating β-catenin and specific downstream target genes involved in cell cycle control and neuronal differentiation.

DISCUSSION

Here, we demonstrate a unique role for Wnt7a signaling in multiple steps of neurogenesis, from neural progenitor cell cycle progression to neuronal differentiation and maturation in the hippocampus of adult mouse brains. We show that loss of Wnt7a expression reduced neural stem cell self-renewal, increased the rate of cell cycle exit in neural progenitors, and inhibited hippocampal dentate neuron production and maturation.

Extensive studies have been performed to determine the role of Wnt7a in axon development and guidance, as well as synapse formation and maintenance (18–23). However, much less is known about the role of Wnt7a in the early steps of neurogenesis. In this study, we show that Wnt7a is important for neural stem cell self-renewal and neural progenitor cell cycle progression. In addition, we demonstrate that Wnt7a plays a critical role in neuronal differentiation and maturation. Deletion of Wnt7a expression led to dramatically reduced numbers of BrdU^{+} DCX^{+} newborn neurons in the hippocampal dentate gyrus of adult mouse brains. Moreover, the dentate granule neurons in Wnt7a$^{-/-}$ mouse brains exhibited dramatically impaired dendritic arborization, indicating a critical role for Wnt7a in dendritic development of hippocampal neurons.

Both Wnt7a and Wnt7b are expressed in the hippocampus (14, 19, 21, 44, 45). This study provides evidence that Wnt7a plays a critical role in dendritic arborization of dentate granule neurons. Both dendritic length and complexity were reduced dramatically in the dentate granule neurons of Wnt7a$^{-/-}$ mice and in neurons transduced with Wnt7a siRNA. Interestingly, Wnt7b also increases dendritic arborization in hippocampal neurons (45). Exposure of cultured hippocampal neurons to Wnt7b-conditioned medium increases neurite length and branching of these neurons (45). The role of Wnt signaling in dendritic development is further supported by observations that modulating other components in the Wnt pathway, including β-catenin and the scaffolding protein Dvl, also regulates dendritic development (45, 46). β-Catenin overexpression increases dendritic arborization (46), whereas Dv1-deficient neurons exhibit much less complex dendrites (45).

In this study, we show that Wnt7a regulates neural stem/progenitor cell proliferation and neuronal differentiation through the canonical Wnt–β-catenin pathway. In proliferating neural stem/progenitor cells, Wnt7a activates the expression of cyclin D1, a downstream target gene of β-catenin (37). Cotransduction of either constitutively active β-catenin or cyclin D1 increased the proliferation of neural stem/progenitor cells that was reduced by Wnt7a knockdown, providing strong evidence that Wnt7a stimulates neural stem/progenitor cell proliferation by activating β-catenin and its downstream target gene cyclin D1. Of interest to us, β-catenin preferentially bound to the promoters of genes involved in cell cycle control or neuronal differentiation in response to different cues. When neural stem/progenitor cells were induced to differentiate into neurons, β-catenin dissociated from the cyclin D1 promoter and bound instead to the Ngn2 promoter to activate Ngn2 expression. Together with a previous observation that overexpression of β-catenin upregulates an Ngn2 reporter gene (43), our ChIP assay data showing the binding of β-catenin to the Ngn2 promoter indicate that Ngn2 is a direct downstream target gene of β-catenin. Cotransduction of either the constitutively active β-catenin or Ngn2 restored neuronal differentiation and maturation that were impaired by Wnt7a siRNA, supporting the idea that Wnt7a promotes neuronal differentiation and maturation by activating the β-catenin–Ngn2 pathway.

In summary, we have demonstrated that Wnt7a plays an important role in multiple steps of neurogenesis, ranging from neural stem cell self-renewal and neural progenitor cell cycle progression to neuronal differentiation and maturation. Wnt7a regulates these processes by activating β-catenin and its downstream target genes that are involved in either cell cycle control or neuronal differentiation.

ACKNOWLEDGMENTS

We thank M. Morgan for expert editing.

This work was supported by NIH NINDS R01 NS059546 and RC1 NS068370 and California Institute for Regenerative Medicine grants TR2-01832 and RB4-06277.

REFERENCES

1. **Gage FH.** 2000. Mammalian neural stem cells. Science **287**:1433–1438.
2. **Chenn A, Walsh CA.** 2002. Regulation of cerebral cortical size by control of cell cycle exit in neural precursors. Science **297**:365–369.
3. **Lee SM, Tole S, Grove E, McMahon AP.** 2000. A local Wnt-3a signal is required for development of the mammalian hippocampus. Development **127**:457–467.
4. **Viti J, Gulacsi A, Lillien L.** 2003. Wnt regulation of progenitor maturation in the cortex depends on Shh or fibroblast growth factor 2. J. Neurosci. **23**:5919–5927.
5. **Yu HM, Liu B, Costantini F, Hsu W.** 2007. Impaired neural development caused by inducible expression of Axin in transgenic mice. Mech. Dev. **124**:146–156.
6. **Zechner D, Fujita Y, Hulsken J, Muller T, Walther I, Taketo MM, Crenshaw EB, III, Birchmeier W, Birchmeier C.** 2003. Beta-catenin signals regulate cell growth and the balance between progenitor cell expansion and differentiation in the nervous system. Dev. Biol. **258**:406–418.
7. **Zhou CJ, Zhao C, Pleasure SJ.** 2004. Wnt signaling mutants have decreased dentate granule cell production and radial glial scaffolding abnormalities. J. Neurosci. **24**:121–126.
8. **Prajerova I, Honsa P, Chvatal A, Anderova M.** 2010. Distinct effects of sonic hedgehog and Wnt-7a on differentiation of neonatal neural stem/progenitor cells in vitro. Neuroscience **171**:693–711.

9. **Kalani MY, Cheshier SH, Cord BJ, Bababeygy SR, Vogel H, Weissman IL, Palmer TD, Nusse R.** 2008. Wnt-mediated self-renewal of neural stem/progenitor cells. Proc. Natl. Acad. Sci. U. S. A. **105**:16970–16975.
10. **Adachi K, Mirzadeh Z, Sakaguchi M, Yamashita T, Nikolcheva T, Gotoh Y, Peltz G, Gong L, Kawase T, Alvarez-Buylla A, Okano H, Sawamoto K.** 2007. Beta-catenin signaling promotes proliferation of progenitor cells in the adult mouse subventricular zone. Stem Cells **25**:2827–2836.
11. **Hirabayashi Y, Itoh Y, Tabata H, Nakajima K, Akiyama T, Masuyama N, Gotoh Y.** 2004. The Wnt/beta-catenin pathway directs neuronal differentiation of cortical neural precursor cells. Development **131**:2791–2801.
12. **Kuwabara T, Hsieh J, Muotri A, Yeo G, Warashina M, Lie DC, Moore L, Nakashima K, Asashima M, Gage FH.** 2009. Wnt-mediated activation of NeuroD1 and retro-elements during adult neurogenesis. Nat. Neurosci. **12**:1097–1105.
13. **Lie DC, Colamarino SA, Song HJ, Desire L, Mira H, Consiglio A, Lein ES, Jessberger S, Lansford H, Dearie AR, Gage FH.** 2005. Wnt signalling regulates adult hippocampal neurogenesis. Nature **437**:1370–1375.
14. **Qu Q, Sun G, Li W, Yang S, Ye P, Zhao C, Yu RT, Gage FH, Evans RM, Shi Y.** 2010. Orphan nuclear receptor TLX activates Wnt/beta-catenin signalling to stimulate neural stem cell proliferation and self-renewal. Nat. Cell Biol. **12**:31–40.
15. **Parr BA, McMahon AP.** 1995. Dorsalizing signal Wnt-7a required for normal polarity of D-V and A-P axes of mouse limb. Nature **374**:350–353.
16. **Miller C, Sassoon DA.** 1998. Wnt-7a maintains appropriate uterine patterning during the development of the mouse female reproductive tract. Development **125**:3201–3211.
17. **Parr BA, McMahon AP.** 1998. Sexually dimorphic development of the mammalian reproductive tract requires Wnt-7a. Nature **395**:707–710.
18. **Ahmad-Annuar A, Ciani L, Simeonidis I, Herreros J, Fredj NB, Rosso SB, Hall A, Brickley S, Salinas PC.** 2006. Signaling across the synapse: a role for Wnt and Dishevelled in presynaptic assembly and neurotransmitter release. J. Cell Biol. **174**:127–139.
19. **Cerpa W, Godoy JA, Alfaro I, Farias GG, Metcalfe MJ, Fuentealba R, Bonansco C, Inestrosa NC.** 2008. Wnt-7a modulates the synaptic vesicle cycle and synaptic transmission in hippocampal neurons. J. Biol. Chem. **283**:5918–5927.
20. **Ciani L, Boyle KA, Dickins E, Sahores M, Anane D, Lopes DM, Gibb AJ, Salinas PC.** 2011. Wnt7a signaling promotes dendritic spine growth and synaptic strength through Ca(2)/calmodulin-dependent protein kinase II. Proc. Natl. Acad. Sci. U. S. A. **108**:10732–10737.
21. **Gogolla N, Galimberti I, Deguchi Y, Caroni P.** 2009. Wnt signaling mediates experience-related regulation of synapse numbers and mossy fiber connectivities in the adult hippocampus. Neuron **62**:510–525.
22. **Hall AC, Lucas FR, Salinas PC.** 2000. Axonal remodeling and synaptic differentiation in the cerebellum is regulated by WNT-7a signaling. Cell **100**:525–535.
23. **Lucas FR, Salinas PC.** 1997. WNT-7a induces axonal remodeling and increases synapsin I levels in cerebellar neurons. Dev. Biol. **192**:31–44.
24. **Shi Y, Lie CD, Taupin P, Nakashima K, Ray J, Yu RT, Gage FH, Evans RM.** 2004. Expression and function of orphan nuclear receptor TLX in adult neural stem cells. Nature **427**:78–83.
25. **Kim JY, Duan X, Liu CY, Jang MH, Guo JU, Pow-anpongkul N, Kang E, Song H, Ming GL.** 2009. DISC1 regulates new neuron development in the adult brain via modulation of AKT-mTOR signaling through KIAA1212. Neuron **63**:761–773.
26. **Smrt RD, Eaves-Egenes J, Barkho BZ, Santistevan NJ, Zhao C, Aimone JB, Gage FH, Zhao X.** 2007. Mecp2 deficiency leads to delayed maturation and altered gene expression in hippocampal neurons. Neurobiol. Dis. **27**:77–89.
27. **Li W, Sun G, Yang S, Qu Q, Nakashima K, Shi Y.** 2008. Nuclear receptor TLX regulates cell cycle progression in neural stem cells of the developing brain. Mol. Endocrinol. **22**:56–64.
28. **Mylius J, Brosch M, Scheich H, Budinger E.** 2012. Subcortical auditory structures in the Mongolian gerbil: I. Golgi architecture. J. Comp. Neurol. **521**:1289–1321.
29. **Shimogori T, VanSant J, Paik E, Grove EA.** 2004. Members of the Wnt, Fz, and Frp gene families expressed in postnatal mouse cerebral cortex. J. Comp. Neurol. **473**:496–510.
30. **Ming GL, Song H.** 2011. Adult neurogenesis in the mammalian brain: significant answers and significant questions. Neuron **70**:687–702.
31. **Zhao C, Deng W, Gage FH.** 2008. Mechanisms and functional implications of adult neurogenesis. Cell **132**:645–660.
32. **Kee N, Sivalingam S, Boonstra R, Wojtowicz JM.** 2002. The utility of Ki-67 and BrdU as proliferative markers of adult neurogenesis. J. Neurosci. Methods **115**:97–105.
33. **Scholzen T, Gerdes J.** 2000. The Ki-67 protein: from the known and the unknown. J. Cell. Physiol. **182**:311–322.
34. **DiSalvo CV, Zhang D, Jacobberger JW.** 1995. Regulation of NIH-3T3 cell G1 phase transit by serum during exponential growth. Cell Prolif. **28**:511–524.
35. **Zhao C, Sun G, Li S, Lang M, Yang S, Li W, Shi Y.** 2010. microRNA let-7b regulates neural stem cell proliferation and differentiation by targeting nuclear receptor TLX signaling. Proc. Natl. Acad. Sci. U. S. A. **107**:1876–1881.
36. **Adams JC.** 1979. A fast, reliable silver-chromate Golgi method for perfusion-fixed tissue. Stain Technol. **54**:225–226.
37. **Tetsu O, McCormick F.** 1999. Beta-catenin regulates expression of cyclin D1 in colon carcinoma cells. Nature **398**:422–426.
38. **Ma Q, Kintner C, Anderson DJ.** 1996. Identification of neurogenin, a vertebrate neuronal determination gene. Cell **87**:43–52.
39. **Sommer L, Ma Q, Anderson DJ.** 1996. Neurogenins, a novel family of atonal-related bHLH transcription factors, are putative mammalian neuronal determination genes that reveal progenitor cell heterogeneity in the developing CNS and PNS. Mol. Cell. Neurosci. **8**:221–241.
40. **Thoma EC, Wischmeyer E, Offen N, Maurus K, Siren AL, Schartl M, Wagner TU.** 2012. Ectopic expression of neurogenin 2 alone is sufficient to induce differentiation of embryonic stem cells into mature neurons. PLoS One **7**:e38651. doi:10.1371/journal.pone.0038651.
41. **Kouzarides T.** 2007. Chromatin modifications and their function. Cell **128**:693–705.
42. **Li B, Carey M, Workman JL.** 2007. The role of chromatin during transcription. Cell **128**:707–719.
43. **Israsena N, Hu M, Fu W, Kan L, Kessler JA.** 2004. The presence of FGF2 signaling determines whether beta-catenin exerts effects on proliferation or neuronal differentiation of neural stem cells. Dev. Biol. **268**:220–231.
44. **Davis EK, Zou Y, Ghosh A.** 2008. Wnts acting through canonical and noncanonical signaling pathways exert opposite effects on hippocampal synapse formation. Neural Dev. **3**:32. doi:10.1186/1749-8104-3-32.
45. **Rosso SB, Sussman D, Wynshaw-Boris A, Salinas PC.** 2005. Wnt signaling through Dishevelled, Rac and JNK regulates dendritic development. Nat. Neurosci. **8**:34–42.
46. **Yu X, Malenka RC.** 2003. Beta-catenin is critical for dendritic morphogenesis. Nat. Neurosci. **6**:1169–1177.